



Cite this: DOI: 10.1039/c5pp00361j

## Application of spectroscopic and theoretical methods in the studies of photoisomerization and photophysical properties of the push–pull styryl-benzimidazole dyes†

B. Jędrzejewska,<sup>\*a</sup> B. Ośmiałowski<sup>a</sup> and R. Zaleśny<sup>b,c</sup>

The synthesis and spectroscopic properties of a series of substituted 1,3-dimethyl-2-aminostyrylbenzimidazolium iodides are described and discussed. The products were identified by NMR, IR and UV-Vis spectroscopy and elemental analysis. Their electronic absorption and fluorescence band positions are affected by the character of the substituent and by the solvent polarity. The fluorescence decay of the dyes shows two lifetimes interpreted in terms of emission from two forms of the dye in the excited state. Moreover, the photochemical *trans* → *cis* isomerization is reported for these compounds. It occurs from the first excited singlet state of the *trans* isomer to the *cis* isomer following a *trans*-S<sub>0</sub> → S<sub>1</sub> excitation. The electron-donating character of the substituent in a styrene moiety is one of the crucial factors influencing the photoisomerization process. The structure of the *cis* isomer was established by <sup>1</sup>H and <sup>15</sup>N NMR. Experimental studies are supported by the results of quantum chemical calculations.

Received 1st October 2015,  
Accepted 4th December 2015

DOI: 10.1039/c5pp00361j

www.rsc.org/pps

## Introduction

It has become clear that the development of molecular and supramolecular electronics, light harvesting and photocatalysis would greatly benefit from the design and synthesis of organic, electroactive and photoactive materials.<sup>1</sup> Organic molecules are already utilized in optoelectronic devices based on electroluminescence, in photoconductors, light emitting devices (LED), solid-state lasers,<sup>2,3</sup> biochemical fluorescent technology and non-linear optics.<sup>4–6</sup> Among organic functional materials, compounds possessing electron-donating (D) and electron-accepting (A) groups on opposite sides of a  $\pi$ -conjugated linker are very important.

Generally, there are two kinds of D–A systems: molecular complexes with intermolecular charge transfer, which are

usually encountered in bulk heterojunction solar cells for instance, and D–A systems joined by covalent bonds exhibiting the intramolecular charge transfer (ICT) within molecules.<sup>7</sup> The photochemical and photophysical properties of the intramolecular D–A systems depend on the excited-state processes that occur after absorption of a photon (interaction with solvent molecules, rotation about single bonds, photoisomerization *etc.*). After excitation, the generated excitons are stabilized and further separated because of the extended conjugation ( $\pi$ -conjugated spacer). In such molecules rapid electron transfer from D to A takes place.<sup>7</sup> Thus, the properties of molecules of D– $\pi$ -A type can be readily changed by modifying the donors or/and acceptors.<sup>1</sup> Regarding the acceptor side, several heterocyclic moieties were described, *i.e.*: quinoline, dimethylindoline, benzoxazole, benzothiazole or benzimidazole.<sup>8,9</sup> Among these the benzimidazole moiety is very useful in the synthesis of such molecules. This heterocycle plays an important role in, for instance, the medical field. The pharmacological activities of benzimidazole such as antiviral, anti-ulcer, antihypertension, and anticancer properties are well documented.<sup>7</sup> Benzimidazole derivatives and their metal complexes<sup>10,11</sup> have been extensively investigated *e.g.* due to their prominence in studies on the interaction of a transition metal complex with nucleic acids.<sup>12</sup> They were also used in determining the mechanism of metal ion toxicity.<sup>13</sup> Furthermore, the benzimidazole derivatives were applied as chromophores with high extinction coefficient, readily tunable absorption wave-

<sup>a</sup>Faculty of Chemical Technology and Engineering, UTP University of Science and Technology, Seminaryjna 3, 85-326 Bydgoszcz, Poland. E-mail: beata@utp.edu.pl

<sup>b</sup>Department of Chemistry, Faculty of Natural Sciences, Matej Bel University, Tajovského 40, 974 01 Banská Bystrica, Slovak Republic

<sup>c</sup>Faculty of Chemistry, Wrocław University of Technology, Wyb. Wyspiańskiego 27, PL-50370 Wrocław, Poland

† Electronic supplementary information (ESI) available: Figures giving <sup>1</sup>H and <sup>13</sup>C NMR and IR spectra of dyes 1–9, HPLC chromatograms, computational details including the optimized geometries (Cartesians) of molecule 1, changes in <sup>1</sup>H NMR spectra of *trans* isomers of compounds 1–9 upon irradiation in DMSO-*d*<sub>6</sub> and fluorescence decays of dye 1 in acetonitrile before and after irradiation. See DOI: 10.1039/c5pp00361j

length, and fluorophoric properties and they are also desirable as large planar synthetic building blocks in supramolecular chemistry.<sup>9</sup>

The important role of benzimidazoles in biomedical research, in organocatalysis, organometallic, and materials chemistry stems from two reasons related to their molecular structure. Firstly, imidazole is a precursor to N-heterocyclic carbenes.<sup>14</sup> Secondly, the benzene ring provides a convenient scaffold for easy functionalization modifying the spatial and electronic characteristics of this moiety. This combination of a reactive carbene center with a modifiable backbone is responsible for increasing attention and the use of benzimidazoles and their N-heterocyclic derivatives.<sup>7,9–13,15</sup>

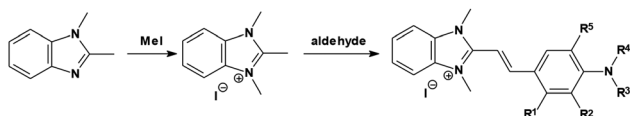
Essentially, styrylbenzimidazole dyes represent stilbene-like structures, with two aromatic moieties and a vinylic C=C double bond, offering the possibility of *trans* → *cis* isomerism. Thus, one should expect styrylbenzimidazole dyes to exist in *trans* and/or *cis* configurations as well as in two resonance structures<sup>16</sup> that should be taken into account when analyzing their properties. It should be emphasized that a quinoid structure might also be considered as an ICT state. In principle the *trans* and quinoid structures can be treated as mesomeric resonance structures, with the positive charge localized on different nitrogen atoms, *i.e.* on the benzimidazole nitrogen in the case of the *trans* isomer and on the substituent's nitrogen atom (*vide infra*) in the quinoid form.<sup>17,18</sup> Therefore, to gain an insight into the electronic properties of the ground and excited states of these dyes it is necessary to collect experimental spectroscopic data.

In this study, we describe the synthesis and perform an analysis of the structure–property relationship for hemicyanine dyes based on a benzimidazole skeleton. We also explore the essential aspects of the *trans* → *cis* photoisomerization for these dyes. It is worth mentioning that a similar photoisomerization was recently described<sup>19–21</sup> also in combination with the supramolecular chemistry approach.

## Experimental section

### Synthetic procedure

In the present study we have followed the synthetic method (Scheme 1) described earlier.<sup>22–24</sup> 2-[4-(*N,N*-dialkylamino)-styryl]-1,3-dimethyl-benzimidazolium iodides were obtained by refluxing (4–6 hours) an appropriate amount of *p*-aminobenzaldehyde (0.01 mol) with 1,2,3-trimethylbenzimidazolium iodide (0.01 mol) in methanol (20 mL) in the presence of piperidine (a few drops). The precipitate formed after cooling down the reaction mixture was filtered out and recrystallized



**Scheme 1** General route for the styrylbenzimidazolium dye synthesis.

from ethanol or methanol. The purity of the dyes under study was checked by thin layer chromatography on aluminum oxide IB-F gel, eluting with a mixture of chloroform and ethanol (5 : 2 v/v).

### Materials and methods

The following solvents, purchased from either Aldrich or Lancaster Chemical Co., were used for spectroscopic measurements: acetonitrile (MeCN), *N,N*-dimethylformamide (DMF), acetone (AcMe), 1-methyl-2-pyrrolidone (MP), tetrahydrofuran (THF), ethylene glycol dimethyl ether (EGDME), propionitrile (EtCN), toluene and benzene. Absorption and emission spectra were recorded at room temperature using a Shimadzu UV-Vis Multispec-1501 spectrophotometer and a Hitachi F-4500 spectrofluorometer, respectively. The concentration of the dye in solvents of different polarities was  $1.0 \times 10^{-5}$  M and  $1.0 \times 10^{-6}$  M for absorption and fluorescence measurements, respectively. The fluorescence quantum yields of the dyes were calculated using eqn (1).

$$\Phi_{\text{dye}} = \Phi_{\text{ref}} \frac{I_{\text{dye}} A_{\text{ref}} n_{\text{dye}}^2}{I_{\text{ref}} A_{\text{dye}} n_{\text{ref}}^2} \quad (1)$$

where:  $\Phi_{\text{ref}}$  is the fluorescence quantum yield of the reference (Coumarin 1;  $\Phi_{\text{ref}} = 0.64$  (ref. 25)) sample in ethanol,  $A_{\text{dye}}$  and  $A_{\text{ref}}$  are the absorbances of the dye and reference samples at the excitation wavelengths ( $A \approx 0.1$  at 404 nm),  $I_{\text{dye}}$  and  $I_{\text{ref}}$  are the integrated emission intensities of the dyes and reference samples,  $n_{\text{dye}}$  and  $n_{\text{ref}}$  are the refractive indices of the solvents used for the dyes and the reference, respectively.

The fluorescence lifetimes were measured using an Edinburgh Instruments single-photon counting system (FLS920P Spectrometers). The apparatus utilizes a picosecond diode laser for the excitation generating pulses of about 55 ps at 375 nm. The dyes were studied at concentrations at which they exhibit similar absorbance at 375 nm (0.2–0.3 in the 10 mm cell). The fluorescence decays were fitted to two-exponential functions. The average lifetime,  $\tau_{\text{av}}$  is calculated as

$$\tau_{\text{av}} = \frac{\sum \tau_i \alpha_i}{\sum \alpha_i} \quad (2)$$

where  $\alpha_i$  and  $\tau_i$  are the amplitude and lifetime.

The photochemical bleaching process was studied in a quartz cuvette with dimensions  $4 \times 1 \times 1$  cm. In order to ensure complete absorption of light, the cuvette was placed in a horizontal position and irradiated with diode-pumped solid state (DPSS) laser light ( $\lambda_{\text{EM}} = 408$  nm; intensity 20 mW) (or xenon lamp equipped with monochromator,  $\lambda_{\text{EM}} = 280$  nm) through the bottom wall (the optical path length = 4 cm). The solution was stirred during irradiation. The photobleaching quantum yield was determined using the following formula:

$$\Phi_{\text{bl}} = \frac{N_A \cdot c \cdot h \cdot V \cdot \Delta A}{\lambda \cdot \epsilon \cdot t \cdot P \cdot l} \quad (3)$$

where  $N_A$  is the Avogadro's number,  $c$  is the velocity of light under vacuum,  $h$  is the Planck's constant,  $V$  is the reaction

volume,  $\Delta A$  is the absorbance difference at the peak wavelength ( $\lambda$ ) prior and post irradiation,  $t$  is the irradiation time,  $\epsilon$  is the molar absorption coefficient of the dye,  $P$  is the power of absorbed light and  $l$  is the optical path length.

The electronic structure calculations were performed using the Kohn–Sham formulation of the density functional theory using the linear response polarizable continuum model (LR-PCM<sup>26</sup>). For a recent comparative study of continuum solvation models we refer to the work of Chibani *et al.*<sup>27</sup> Optimization of the ground state geometry was carried out using two exchange–correlation functionals: B3LYP and CAMB3LYP. Vertical excitation energies were computed employing the time dependent density functional theory. For all quantum-chemical calculations the 6-311++G(d,p) basis set was used. All electronic structure calculations were performed using the Gaussian 2009 (revision D01) program.<sup>28</sup>

## Results and discussion

### Molecular design and synthetic procedures

Nine hemicyanine dyes (Fig. 1) have been synthesized by the reaction (Knoevenagel condensation) of 1,2,3-trimethyl-benzimidazolium iodide with an appropriate amount of *p*-aminobenzaldehyde.<sup>22–24</sup> It is fair to mention that an alternative method (solvent-free microwave irradiation) of the hemicyanine synthesis was described by Lan-Ying Wang *et al.*<sup>29,30</sup> The <sup>1</sup>H and <sup>13</sup>C NMR chemical shift data are in agreement with the dyes structures. The two characteristic doublets related to vinyl protons in a *trans* conformation (<sup>3</sup>*J*<sub>H,H</sub> = 15–16 Hz) are localized roughly at 7 and 8 ppm. Detailed analytical and spectroscopic data for the novel styrylbenzimidazolium dyes are available in the ESI.†

### UV-Vis spectroscopic properties

The spectroscopic data of dyes 1–9 in nine solvents of different polarities are collected in Table S1.† All hemicyanine dyes studied in this work show a characteristic absorption band

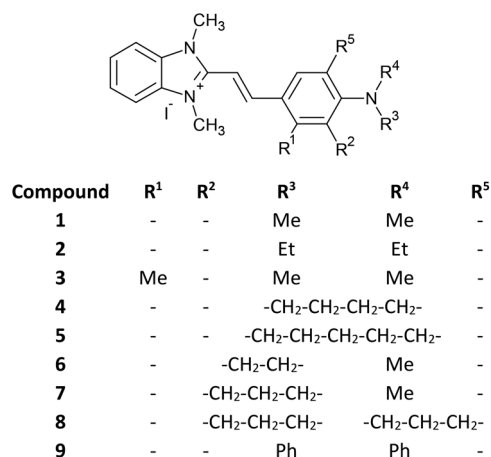


Fig. 1 Dyes studied.

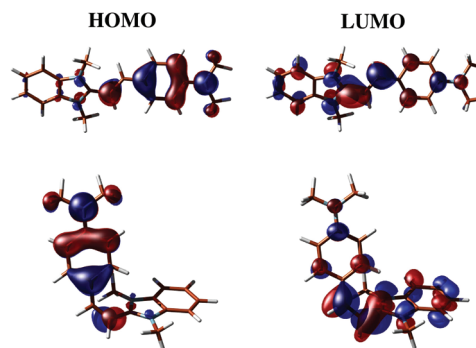


Fig. 2 Frontier orbitals involved in the lowest-energy excitation for *trans*-1 (top) and *cis*-1 (bottom) in DMF solvent.

with the maximum at the range 418–475 nm and a corresponding, clearly Stokes-shifted, emission band ( $\lambda_{\text{EX}} = 404$  nm). The broad absorption bands correspond to the  $\pi \rightarrow \pi^*$  ICT transition involving the amino nitrogen and the cationic benzimidazolium moiety.<sup>18,22</sup> Indeed, the results of time-dependent density functional calculations for compound 1 (*cf.* Table S2 in ESI†) reveal that the  $\pi \rightarrow \pi^*$  excitation to the lowest-energy state is dominated by the HOMO  $\rightarrow$  LUMO transition. The shape of the two frontier orbitals for *trans*-1 and *cis*-1, shown in Fig. 2, confirms that the density reorganization takes place from dimethylamino to the benzimidazolium moiety. The short-wavelength bands are attributed to the  $\pi \rightarrow \pi^*$  transitions. As an example, the spectra of the dye are shown in Fig. 3. The molar absorption coefficients of the CT bands are in the range 31 200–45 600 M<sup>-1</sup> cm<sup>-1</sup>. The high value of the molar absorption coefficient indicates an extensive conjugation of  $\pi$ -electrons, thus suggesting a planar structure of the dye molecule in its ground state. In fact this is confirmed by the results of calculations.

The selected bond lengths, as predicted by quantum chemistry calculations, for *trans* and *cis* forms are summarized in Table 1. The theoretical calculations show that the bond lengths of the  $\pi$ -spacer show a single–double–single bond

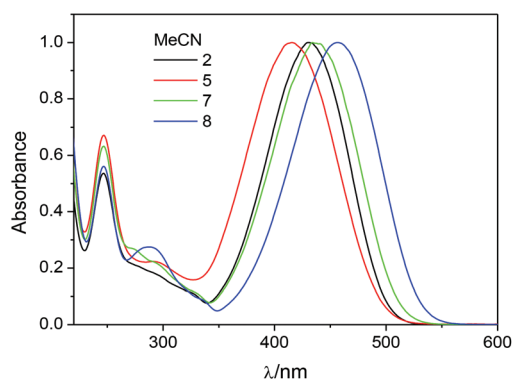


Fig. 3 Normalized electronic absorption spectra of selected hemicyanine dyes (2, 5, 7 and 8 in MeCN at 293 K).

**Table 1** Crucial bond lengths [Å] for optimized structures of **1**

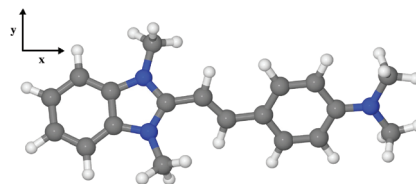
	<i>trans</i>	<i>cis</i>
Imidazole C–CH(=CH–)	1.432	1.449
CH=CH	1.366 <sup>a</sup>	1.362
(–CH=)CH–C <sub>ipso</sub>	1.440	1.448
C <sub>ortho</sub> –C <sub>meta</sub>	1.381	1.382
C <sub>para</sub> –NMe <sub>2</sub>	1.365	1.367

<sup>a</sup> 1.341 in *trans*-4-NMe<sub>2</sub>-cinnamaldehyde,<sup>31</sup> 1.336 in *trans*-4-NMe<sub>2</sub>-C<sub>6</sub>H<sub>4</sub>-*p*-CH=CH–NO<sub>2</sub>,<sup>32</sup> 1.332 in *trans*-4-NMe<sub>2</sub>-C<sub>6</sub>H<sub>4</sub>-*p*-CH=CH-2-(*N*-methylpyridine).<sup>33</sup>

character confirming the ethenic linkage character in the ground state. The values of bond angles between imidazole carbon and the central double bond (and between the central double bond and benzene carbon) are equal to 127.64° (125.65°) for *trans* and 132.66° (129.3°) for *cis* forms, respectively. The torsional angle of C–CH=CH–C equals 179.57° for the *trans* form, thus confirming its planarity in the ground state. The corresponding angle for the *cis* isomer is –11.33°.

The absorption spectra of the studied compounds are affected by the type of dialkyl(aryl)amino group in the dye molecule. In all the solvents the maximum absorption positions (Table S1†) differ in some cases up to 40 nm and this indicates that the energy of electronic transition substantially depends on the structure of the electron-donating moiety. It can be seen that the replacement of the NMe<sub>2</sub> group (dye **1**) by the NEt<sub>2</sub> one (dye **2**) shifts the absorption band toward a longer wavelength by about 10 nm. Additionally, a bathochromic effect is observed when the methyl group is introduced in the *ortho* position to the central double bond (compound **3**) or upon elimination of the free rotation of the dialkylamino group by the bridging (compounds **6**, **7** and **8**). The absorption spectra of the largely bridged compound (**8**) are the most shifted to lower energies. This is probably due to reduction of conformational flexibility in the ground state and it is connected with an increasingly rigidized molecular skeleton.<sup>8,17,34</sup> On the other hand, the blue shift of the CT absorption band appears when the alkylamino group is twisted because the coplanar conformation decreases the probability of radiative transitions.

The UV-Vis absorption spectra recorded in solvents of different polarities show weak solvatochromism. Upon increasing the solvent polarity, the CT absorption band is slightly blue-shifted as for instance the change of the solvent from benzene to DMF in the case of **1** changes the maximum absorption wavelength from 438 nm to 424 nm. The results indicate that these molecules might possess fairly similar polarities between the excited state and the ground state and thus the energy gap is barely influenced by the increasing polarity of the solvent.<sup>35</sup> In order to gain a deeper insight into the polarity changes upon photoexcitation to the lowest-energy  $\pi \rightarrow \pi^*$  excited state, we performed quantum chemistry calculations for the *trans* isomer of compound **1**. Note that unlike dipole moment components in the ground and excited states,

**Fig. 4** Orientation of *trans*-**1** in Cartesian coordinate system for the ground- and excited-state dipole moment calculations.

only their differences are translationally invariant for a charged system. The orientation of *trans*-**1** for property calculations is shown in Fig. 4. The dipole moment change upon photoexcitation along the conjugation pathway, *i.e.* along the *x* direction, is an order of magnitude larger than that for the other directions. The value of  $\Delta\mu_x$  for *trans*-**1** is 8.6 D and 10.1 D in benzene and DMF, respectively. Thus, as already mentioned, one observes an increase of  $\Delta\mu$  with increasing solvent polarity.

As in the case of electronic absorption spectra, the structure of the electron donor group and solvent polarity also affect the position of the emission band. The rigidity and planarization of the amino group lead to the red shift in the fluorescence (see Table S1†). A solvent change from benzene to acetonitrile causes a bathochromic shift roughly by few nanometers for its fluorescence band, *e.g.* the maximum emission peak for **1** is at 541 nm in benzene and at 546 nm in MeCN. Only in the case of dye **9** a more pronounced effect is observed. Solvent change from benzene to acetonitrile causes a bathochromic shift in fluorescence maximum equal to 120 nm. In the same compound the absorption peak position shifts to the blue only by 10 nm. For *N,N*-diphenylamine-substituted dye (**9**) a clear red-shift of the fluorescence spectra with increasing polarity of the solvents indicates the occurrence of an intramolecular charge transfer process from the electron-donating triphenylamine moiety to the electron-accepting benzimidazole moiety. As a result the excited state energy decreased with increasing polarity of the solvents due to enhanced solvent-solute dipole-dipole interactions, and the energy gap between the ground state and excited state declined, which explains the sensitivity of the emission spectra of the compound toward solvent polarity.<sup>34,35</sup>

Generally, data collected in Table S1† reveal that the long wavelength absorption band undergoes a hypsochromic shift as the solvent polarity increases whereas there is a bathochromic shift of the fluorescence band, with an increase of the Stokes shift as the solvent polarity increases (Fig. S1†). On changing the solvent from nonpolar to polar, the change in the Stokes shift equals *ca.* 4400 cm<sup>-1</sup> for **9** and *ca.* 1000 cm<sup>-1</sup> for other dyes, respectively. The large value of the Stokes shift indicates that the excited-state geometry differs significantly from that of the ground state.<sup>36,37</sup>

Table S1† shows that the Stokes shifts of the studied dyes are large (>3000 cm<sup>-1</sup>). Presumably, this can be linked to the extensive ICT across the molecule, which is facilitated by the

presence of a typical D- $\pi$ -A structure. An increase in the Stokes shift with increasing solvent polarity indicates an increase in the dipole moment upon excitation.<sup>36,37</sup>

To gain a further insight into the emission process the fluorescence decay profiles were recorded by using the time correlated single-photon counting system. The samples were excited at 375 nm and the emissions were followed at 550 nm. The decay curves were fitted to two-exponential decay and the lifetimes were extracted from the measured decay curves by deconvolution of the instrument response function. The fluorescence decay profile of selected dyes is shown in Fig. 5. The results of lifetime measurements are summarized in Table 2.

The two-exponential character of the decays is consistent with the observations of Röcker *et al.*<sup>38</sup> and Rettig *et al.*<sup>39</sup> for similar compounds. From their work it is known that hemicyanine dyes exist as a mixture of rotamers. Rettig *et al.* investigation<sup>39</sup> shows that single bonds adjacent to the ethylenic group lead to low lying twisted intramolecular charge transfer states with possibly emissive properties while the twist of the dimethylamino group leads to an energetically higher lying twisted intramolecular charge transfer state, unlikely to be populated thermally.

On the other hand, twisting around the central bond leads to an excited state considerably lower in energy than the planar one. This state possesses a nonemissive character because of the small energy gap between the ground and excited states.<sup>39</sup> So, the emitting structures at room temperature are linked to conformations with close to planar geometries. In this approach, the dominant component in fluorescence decay of the studied dyes can be attributed to the emission from the *trans* isomer.<sup>18</sup> The short lifetime ( $\tau_1$ ) in

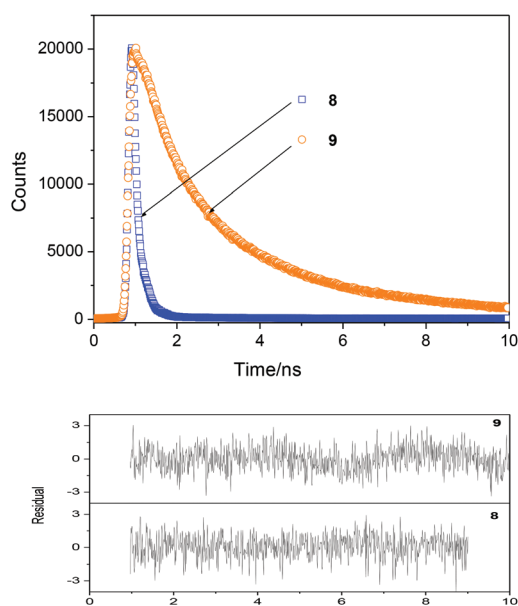


Fig. 5 Fluorescence decays of 8 and 9 dyes (weighted residuals are shown in the bottom panels) in AcOEt–NMP mixture (10 : 1 v/v) ( $A \approx 0.2$ – $0.3$  in the 10 mm cell,  $\lambda_{EX} = 375$  nm,  $\lambda_{EM} = 550$  nm, at r.t.).

Table 2 Fluorescence quantum yield ( $\Phi_f$ ) determined with the use of Coumarin 1 in ethanol ( $\Phi = 0.64$  (ref. 25)) as reference ( $A \approx 0.1$  in the 10 mm cell at  $\lambda_{EX} = 404$  nm at r.t.) and fluorescence lifetime results ( $A \approx 0.2$ – $0.3$  in the 10 mm cell,  $\lambda_{EX} = 375$  nm, and  $\lambda_{EM} = 550$  nm, at r.t.) of hemicyanine dyes 1–9

Dye	$\Phi_f$ (%)	$\tau_1$ (ps)	$\tau_2$ (ps)	$\alpha_1$	$\alpha_2$	$\tau_{av}$ (ps)	$\chi^2$
AcOEt – MP mixture (10 : 1 v/v)							
1	0.81	65	1719	96.7	3.3	120	1.28
2	0.95	67	2694	81.3	18.7	558	1.06
3	0.38	53	2436	90.5	9.5	279	1.25
4	1.13	71	1411	92.2	7.8	176	1.22
5	1.32	79	1887	94.5	5.5	178	1.06
6	0.70	69	960	96.8	3.2	98	1.29
7	0.75	66	1194	98.8	1.2	79	1.35
8	1.22	80	1046	98.4	1.6	96	1.08
9	14.73	107	2372	69.5	30.5	798	1.10
MeCN							
1	0.73	36	1040	99.8	0.2	38	1.81
2	0.95	38	1249	99.3	0.7	46	1.77
3	0.42	31	729	98.5	1.5	41	1.08
4	1.02	38	1421	99.2	0.8	49	1.83
5	1.14	41	872	99.9	0.1	41	1.02
6	0.66	35	1213	99.4	0.6	40	1.86
7	0.98	39	1105	99.6	0.4	43	1.52
8	0.80	37	1326	98.9	1.1	51	1.42
9	2.71	64	1131	93.7	6.3	131	1.94

this case reflects the fast reaction from the planar Franck-Condon state to a non-emissive partially twisted state (the so-called “phantom” state) which quickly leads to internal conversion to  $S_0$  as a mixture of *trans* + *cis* isomers. The long lifetime component may instead be assigned to the perpendicular quinoid ( $Q_{\perp}$ ) or ICT form, respectively.<sup>17,18,40–44</sup> However, because of the small percentage of long-lived components only the main component of the fluorescence decay curve (above 90%) was selected for further analysis.

The radiative rate constants  $k_r$  and the total nonradiative rate constants  $k_{nr}$  from the singlet-excited state of tested dyes were estimated from the fluorescence quantum yield ( $\Phi_f$ ) and the main lifetime ( $\tau_1$ ) values using well-known equations.<sup>36</sup> Thus, the calculated rate constants are  $k_r = (0.71$ – $13.76) \times 10^8 \text{ s}^{-1}$  and  $k_{nr} = (0.8$ – $3.21) \times 10^{10} \text{ s}^{-1}$  (Table 3). This estimation

Table 3 The radiative ( $k_r$ ) and non-radiative ( $k_{nr}$ ) rate constants with reference to average lifetimes and the rate constants ( $k$ ) and quantum yields ( $\Phi_{bl}$ ) of photobleaching process (*vide infra*) for tested dyes

Dye	$k_r$ ( $10^8 \text{ s}^{-1}$ )		$k_{nr}$ ( $10^{10} \text{ s}^{-1}$ )		$k_{nr}/k_r$		$\Phi_{bl}$	$k$ ( $10^{-4} \text{ s}^{-1}$ )
	A	B	A	B	A	B		
1	1.24	2.02	1.53	2.76	122.8	136.4	0.144	4.75
2	1.42	2.50	1.48	2.61	104.1	104.3	0.148	4.93
3	0.71	1.35	1.88	3.21	263.0	237.3	0.155	5.40
4	1.59	2.69	1.39	2.60	87.5	96.9	0.147	5.34
5	1.67	2.79	1.25	2.41	74.6	86.5	0.137	4.53
6	1.01	1.89	1.44	2.84	142.3	150.0	0.091	4.19
7	1.13	2.52	1.50	2.54	132.6	100.8	0.133	4.45
8	1.51	2.17	1.23	2.68	81.1	123.8	0.119	4.02
9	13.76	4.24	0.80	1.52	5.8	35.9	0.002	0.10

indicates that for the tested hemicyanines the non-radiative transition rate is at least two orders of magnitude faster than the radiative rate.

The results of spectroscopic and lifetime measurements indicate the existence of multiple species of the styrylbenzimidazolium dye in organic solvents. In the case of hemicyanine dyes, the presence of a positive charge at two different types of nitrogens in the molecule (two resonant forms) may cause that some specific solvents can stabilize these two structures to different extents. The degree of the charge transfer can influence the properties of dyes including the bond order and thus the bond rotational barrier.<sup>16,17,30,34–37,40,41</sup>

### Trans → cis photoisomerization

Due to the presence of the carbon–carbon double bond, the hemicyanine dyes may undergo photoreactions typical of alkenes. The most characteristic reaction is the *trans*–*cis* isomerization. It is obvious that the photophysical properties of such molecules may be dependent on the *trans*–*cis* isomerism. Thus, it is crucial to gain an insight into the photophysics of these dyes.

Irradiation with a laser beam ( $\lambda = 408$  nm, 20 mW) of a solution of **1** prepared in the dark causes a progressive decrease in the absorbance of the long-wavelength band ( $\lambda_{\text{max}}$  initially at 425 nm) with a concomitant increase in the absorbance intensity at *ca.* 280 nm until a stationary state is reached (Fig. 6 top). The sharp isosbestic point at *ca.* 370 nm is evi-

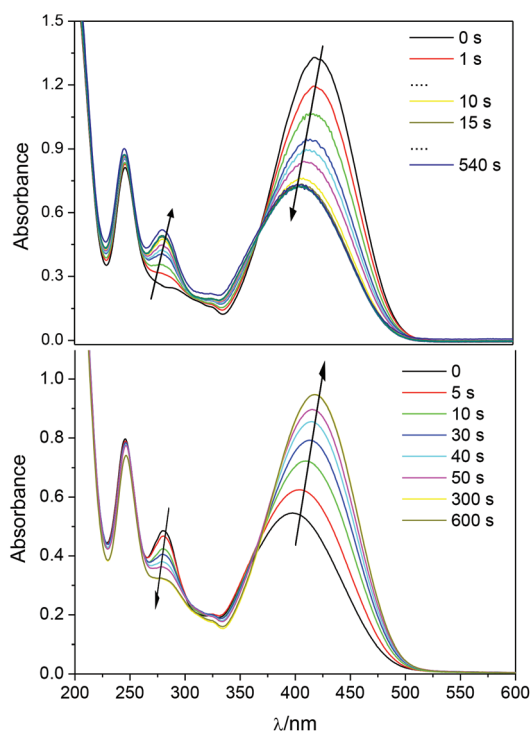


**Fig. 6** The dependence of UV-Vis absorption spectra of **1** in MeCN upon irradiation with DPSS laser beam ( $\lambda = 408$  nm, 20 mW, top) and xenon lamp ( $\lambda = 280$  nm, bottom). Arrows indicate the direction of changes with time of irradiation.

dence for a transformation between two species, but not yet proof for a photoisomerization (any photodegradation could lead to a similar behavior).<sup>16</sup> Once a photostationary state had been reached, we have changed the excitation wavelength to a region where an increase in absorption was observed and irradiated the sample at 280 nm (xenon lamp equipped with a monochromator). The results (Fig. 6 bottom) show a reversal trend: an increase of the main band (around 425 nm) and a decrease of absorption at *ca.* 280 nm.

In order to distinguish the substrate from the product formed after irradiation of the solution NMR analysis was performed. The spectra were recorded for (a) the initial solution prepared in the dark, (b) after heating in the dark and (c) after irradiation (Fig. S2†).

The analysis of  $^1\text{H}$  NMR spectra of **1** in DMSO- $d_6$  indicates that the heating of solution (b) did not cause any changes in the signal position. There are well-separated pairs of doublets for two olefinic protons. The coupling constant  $^3J_{\text{H,H}} = 16.4$  Hz is characteristic for the *trans* configuration. After irradiation to a photostationary state and transition, the proton spectrum of the same solution shows considerable changes in chemical shifts. It becomes evident that for the new pair of doublets the coupling constant is equal to 12.0 Hz, which is in perfect agreement with the *cis* arrangement (the similar is observed in acetonitrile).<sup>45</sup> It follows from the studies of Steiner *et al.*<sup>16</sup> that in the *cis* configuration, as in *cis*-stilbene, two arene rings must be twisted from the coplanar orientation relative to the central double bond. Upon rotation of the aromatic parts of the molecule around the single bonds adjacent to the central double bond,  $\text{H}^{\text{d}}$  and  $\text{H}^{\text{e}}$  (Fig. 7) protons may come into the screening cone of the anisotropic ring current. This would result in different shielding in *cis* and *trans* isomers. Simultaneously, the aryl protons in the *ortho* position to the olefinic spacer ( $\text{H}^{\text{f}}$ ) are located well within the shielding cone of the benzimidazole ring in the *cis* conformation, and thus experience a significant high-field shift. Such an effect is in fact observed.

The additional experiments were focused on the possibility of thermal isomerization of **1**. The following steps were recorded ( $^1\text{H}$  and  $^{15}\text{N}$  spectra) for (1) the parent sample (*trans* form), (2) the sample heated at 80 °C for at least 4 h, (3) the irradiated sample (visible light, r.t., time = 4 h), (4) the re-heated sample that was irradiated before (from step 3, in order to check if the *cis*-to-*trans* thermal isomerization takes place,

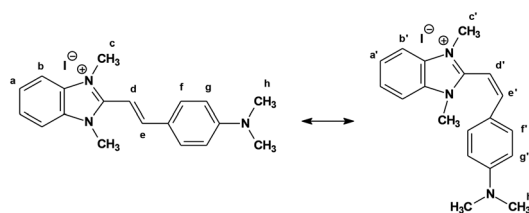


**Fig. 7** The *trans* and *cis* forms of the dye **1**.

80 °C, 3 h). The results are summarized in Table 3, while the stacked spectra are collected in Fig. S2.†

Analysis of the NMR and electronic absorption spectra recorded under various conditions (data presented in the ESI†) indicates that the *trans* isomer is thermally stable but is partially converted to the *cis*-isomer under visible light irradiation. Based on the NMR spectra of **1** recorded for the photostationary state the *trans/cis* photoisomer ratio was calculated by integrating respective peaks corresponding to the vinylic doublets and/or the methyl groups in *cis* and *trans* forms. The re-heated sample (step 4, 3 h at 80 °C) did not exhibit any significant changes in the absorption and NMR spectra. However, the abundance of the *trans* form increased. Thus, a more precise study of the thermal back-reaction was performed. The <sup>1</sup>H NMR spectra of a previously irradiated sample of **1** at r.t., recorded 16 h, 36 h, 39 h and 74 h after heating (see Fig. S3†) show that the peaks attributable to the *cis* isomer decrease in intensity. Signal integration suggests that almost all of the *cis* isomer reverts thermally to the *trans* isomer after 74 h at 373 K (a percent of the remainder *cis* form equals *ca.* 2.8%). This indicates that the *cis*-to-*trans* thermal interconversion is slow and inefficient and this is, most probably, due to the high value of *cis* → *trans* activation energy. Similarly to Mishra *et al.* studies,<sup>46</sup> the photoisomerization of styrylbenzimidazolium iodides follow the non-adiabatic path and occur *via* the perpendicular state. However, in contrast to the neutral molecule,

the *trans* and *cis* isomers of the tested dyes exist only in one conformeric form.

Further, calculations were based on the geometry of *trans* and *cis* forms. The shieldings of the nuclei in **1** were used to calculate the chemical shifts. It is known that the nitrogen atom is sensitive to the environment<sup>47</sup> thus its chemical shift may be a method of choice for distinguishing between two isomeric forms. This is especially true for compounds, which exhibit intramolecular charge transfer. Such charge transfer is dependent on the geometry of the molecule and thus it can be directly linked to the *cis*-*trans* isomerism. The GIAO-based<sup>48,49</sup> calculations yield various chemical shifts for imidazole and NMe<sub>2</sub> group nitrogen atoms in *trans* and *cis* forms (see row *c* in Table 4). Table 5 collects the experimental and calculated <sup>15</sup>N NMR data (with respect to MeNO<sub>2</sub>). The same table contains (in *italic*) the values of the <sup>1</sup>H chemical shifts of methyl groups that gave a cross-peak in <sup>1</sup>H,<sup>15</sup>N HMBC spectra. It is clearly seen that methyl protons are also sensitive to isomerism of **1**.

The differences between experimental and calculated chemical shifts may be related to the fact that under experimental conditions the averaged structure related to thermal motions is observed while in calculations only one conformation, *i.e.* the optimal one, is taken into account. Despite the differences in experimental conditions and model calculations, it is also worth emphasizing that (a) the trends in calculations are preserved with respect to the experimental data and (b) the difference between experimental and calculated values of 10 ppm (<sup>15</sup>N) is less than 3% error on the <sup>15</sup>N scale. Moreover, in experiments the solvent-solute interactions exist and the I<sup>-</sup> anion is present while in calculations the solvent is treated as a continuum and only the organic cation is optimized. However, the calculations reflect the general trends observed in DMSO-*d*<sub>6</sub> solution after irradiation (photoisomerization). In the case of *trans* conformation, the chemical shifts are lower for imidazole nitrogen atoms and higher for the NMe<sub>2</sub> group. The same trend is found based on the results of computations. Finally, both the measured and calculated difference in chemical shifts for NMe<sub>2</sub> and imidazole are larger for the *cis* conformation. This is in agreement with the fact that in the case of *trans* arrangement the charge transfer is more effective than in the case of *cis* form. This enables a higher degree of equalization of shielding the nuclei by electrons.

**Table 4** Results of probing the sample of **1** after heating and irradiation

Step (see text)	<sup>1</sup> H ( <i>trans</i> ) <sup>a</sup>	<sup>15</sup> N ( <i>trans</i> )	<sup>1</sup> H ( <i>cis</i> ) <sup>b</sup>	<sup>15</sup> N ( <i>cis</i> )	% of <i>trans</i> form <sup>c</sup>
1	7.196	-230.7	—	—	100
	7.746	-317.2			
2	7.196	-231.5	—	—	100
	7.744	-317.7			
3	7.197	-230.7	6.400	-225.8	12
	7.742	-317.2	7.525	-319.7	
4	7.197	-231.0	6.399	-226.0	19
	7.742	-318.0	7.525	-320.5	

<sup>a</sup> Chemical shift of the vinylic protons (*trans* doublet with <sup>3</sup>J<sub>H,H</sub> = 16.3 Hz). <sup>b</sup> Chemical shift of the vinylic proton (*cis* doublet with <sup>3</sup>J<sub>H,H</sub> = 12.0 Hz). <sup>c</sup> Ratio based on integration of the vinylic doublets ([*trans*]/[*trans*] + [*cis*]).

**Table 5** The experimental and calculated <sup>15</sup>N NMR data with respect to MeNO<sub>2</sub>

Atom (form)	Exp.	Calcd	Δ <i>trans</i> -to- <i>cis</i> <sup>a</sup>	Δ NMe <sub>2</sub> -to- imidazole N
NMe <sub>2</sub> ( <i>trans</i> )	-317.2 (NMe <sub>2</sub> , 3.04)	-332.7	2.5	86.5
NMe <sub>2</sub> ( <i>cis</i> )	-319.7 (NMe <sub>2</sub> , 2.93)	-336.8	4.1	71.3
Imidazole N ( <i>trans</i> )	-230.7 (CH <sub>3</sub> , 4.10)	-261.4	4.9	93.9
Imidazole N ( <i>cis</i> )	-225.8 (CH <sub>3</sub> , 3.77)	-252.9	8.5	83.9

<sup>a</sup> First and second row represent experimental and calculated (**bold**) values, respectively.

The above presented discussion indicates that the investigated styrylbenzimidazole molecules undergo a photoinduced *trans*-to-*cis* isomerization along the central carbon-carbon double bond. The photochemical conversion from the *trans*-form to the *cis*-form and *vice versa* is induced by absorbed light. The *trans*-form absorbs more light relative to the *cis*-form at 408 nm, while ultraviolet light (280 nm) is mainly absorbed by the *cis*-form.

### Substitution effect and photoisomerization

The kinetics of the photoisomerization was studied by measuring the changes in the area under corresponding peaks in  $^1\text{H}$  NMR spectra as a function of irradiation time (see Fig. S4–S12 in the ESI†). The kinetic equation for the photochemical reaction takes the following form:

$$[\textit{trans}] = [\textit{trans}]_0 \exp(-kt) \quad (4)$$

where  $k$  is the observed rate constant, and  $t$  is the time of irradiation. In what follows we use the logarithmic scale for analysis of the experimental data to obtain  $k$ .

Since all signals in  $^1\text{H}$  NMR spectra for the *trans* and *cis* forms are well separated, small changes in the *trans*:*cis* ratio were readily determined. Fig. 8 compares the kinetic behavior for selected styrylbenzimidazole dyes containing various donor groups. The kinetic data fit well to a mono-exponential func-

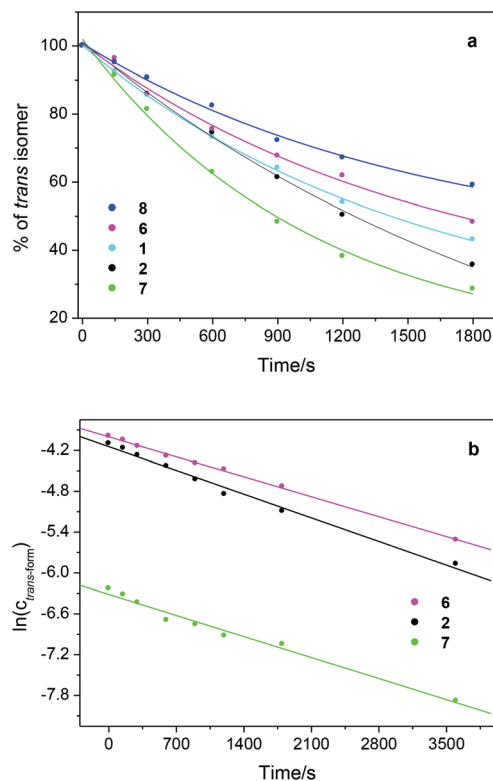


Fig. 8 (a) Changes in abundance of *trans* form during white light irradiation as monitored by  $^1\text{H}$  NMR spectroscopy. (b) Kinetics of styrylbenzimidazole photoisomerization induced by irradiation.

tion, giving the rate constant of *trans*-*cis* photoisomerization ( $k$ ) in  $\text{DMSO}-d_6$ . The obtained data are compiled in Table 2.

The substitution (the structure of the donor part of dyes) has a strong impact on the kinetics of the *trans*-*cis* reaction as seen in Fig. 8. An acceleration of the reaction is achieved by stronger electron-donating groups, while less electron-releasing groups slow down the reaction kinetics. This is in agreement with ICT and the quinoid-like structure, *i.e.* the central vinyl bond has a more singular character with increasing electron-donating ability of a substituent.

To quantify the substitution effect, besides the NMR data, the electronic absorption spectra were also analyzed. The obtained results allow us to calculate the photobleaching quantum yield (Table 2). The photobleaching quantum yields and rate constants of the photochemical process have the smallest values for **9**, while the highest values are observed for compound **3**. The dyes possessing the stiffened  $-\text{NR}_2$  group have much better photostability, whereas the compounds with alkyl groups which are linked to the N position are less stable. The dye with the methyl group in the *meta* position with respect to the  $-\text{NR}_2$  substituent is the least stable. The less electron-releasing group improves photostability compared with the dyes with a stronger electron-donating group which decreases photostability obviously.

The influence of the substitution by various amino groups affecting the rate of the photoisomerization was quantitatively described using the Hammett relationship with known ground-state parameters,  $\sigma$ .<sup>50</sup> Fig. 9 shows the Hammett correlations for the *trans*-*cis* process. Since in **9** some other processes are present (as mentioned above) manifested by much larger Stokes' shifts especially in polar solvents (Table S1†) we performed a correlation with and without this substituent.

The linear Hammett relationship for the investigated reaction shows that a pronounced structure-activity relationship exists for investigated compounds.

A quantitative correlation between the empirically derived Hammett constants and the reaction rates suggests that the type of amino substituent controls the photochemical behavior of the styrylbenzimidazole molecules. Such a correlation was

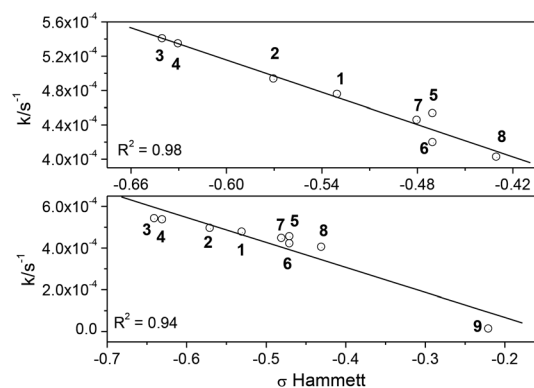


Fig. 9 Hammett correlation for the *trans*-*cis* photoisomerization in **1–8** (top) and **1–9** (bottom) ( $R^2$  correlation coefficient).

earlier observed for other stilbene derivatives.<sup>51–53</sup> The observed substituent effects indicate that the product formation during *trans*–*cis* isomerization of styrylbenzimidazole molecules occurs *via* a transition state (TS) with effective delocalization of a positive charge.<sup>54,55</sup>

The photostability of the hemicyanine dyes is strongly dependent on their chemical structure. The influence of substitution on the photochemical rate is also reflected in fluorescence spectroscopy. Since time-resolved fluorescence is a very sensitive technique to detect multiple emissive species,<sup>36,56</sup> in the present study we carried out such measurements, recording the fluorescence decays of the dye **1** in MeCN solutions, as a function of the monitoring emission wavelength.

As indicated by the time-resolved emission spectra (TRES) constructed based on the emission wavelength dependent fluorescence decays, the fluorescence intensity decreases sharply for the initial time span. During this time, however, there is hardly any shift in the spectral position, as clearly indicated in Fig. 10. These observations are in accordance with our inference that the major contribution in the fluorescence decays is due to the excited *trans*-dye having a reasonably short fluorescence lifetime of *ca.* 0.04 ns in MeCN.

At the long time spans, there is a significant blue shift in the TRANES. This observation evidently indicates that the major emitting species at the latter time span have largely blue-shifted emission spectra in comparison with that of *trans* form. The clearly visible isoemissive point at 500 nm indicates

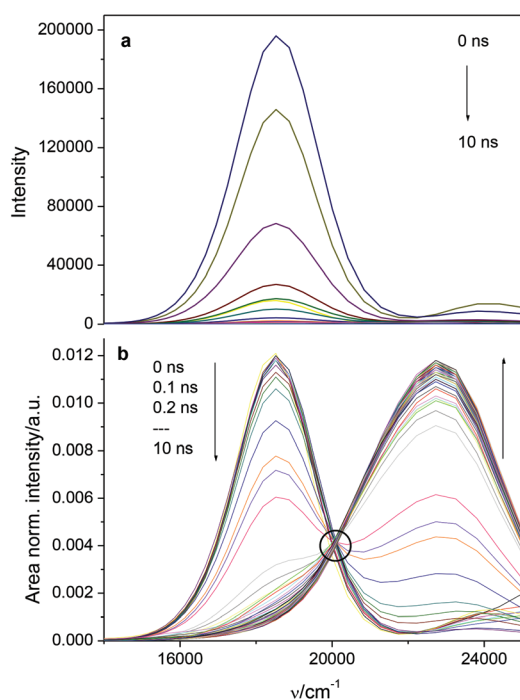


**Fig. 10** (a) Time-resolved emission spectra (TRES) and (b) time-resolved area-normalized emission spectra (TRANES) of **1** in MeCN constructed from the decay transients obtained at different wavelengths.

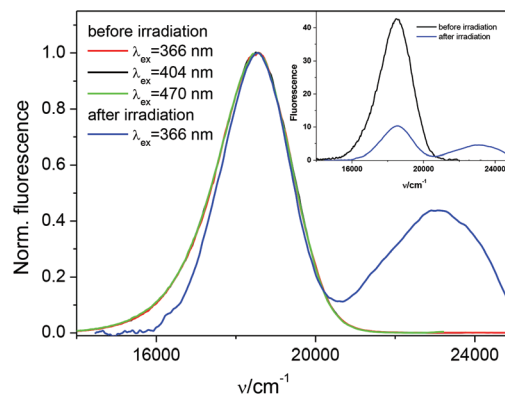


**Fig. 11** Steady-state fluorescence spectra before and after irradiation of diluted solution of **1** in MeCN.

that the emission comes from two species. The blue-shifted low intensity emission in the TRANES might be connected with the *cis* form or more probably come from a locally excited state due to deconjugation.

It is worth mentioning that the same effect was observed in steady-state fluorescence measurements as seen in Fig. 11. Due to difficulty in isolating the sterically hindered isomers we extended our fluorescence studies to include pure *trans* and a mixture of *trans* and *cis* isomers. The *trans* isomer is characterized by a strong component of the short lifetime  $\tau_1$  (see Fig. S13 in the ESI<sup>†</sup>) and fluorescence maximum at 545 nm in MeCN. The fluorescence spectrum of the *trans*–*cis* mixture in MeCN has two maxima, one at 545 nm and the second at 435 nm. The fluorescence intensity of the long-wavelength band decreases, but no shift is observed in that case. The emission decrease indicates the formation of a *cis* isomer after irradiation. In most cases, the *cis* isomers are observed to be either very weakly fluorescent or completely non-fluorescent in nature, mainly because of their fast nonradiative de-excitation rates.<sup>18,39,42–44,57,58</sup> The fluorescence decay of a mixture of *trans* and *cis* isomers of **1** is also two-exponential in MeCN. A steady increase in the long-lived fluorescence lifetime  $\tau_2$  with the increase in population of the *cis* isomer was observed (see Fig. S13 in the ESI<sup>†</sup>). These results suggest that the *cis* isomer converts to the same excited state as that of the *trans*.

To sum up, *trans*-to-*cis* and *cis*-to-*trans* photoisomerization of styrylbenzimidazole molecules occurs through a common intermediate in the excited state, which is the transition state (TS). Presumably, the TS corresponds to a quinoid form with a twist of the two aromatic planes on either side of the double bond.<sup>18,34,37,38</sup>

## Conclusions

The synthetic method described provides an attractive and environmentally friendly pathway to several useful hemicyanine dyes.

Visible light promotes the conversion of the *trans*-isomer of styrylbenzimidazolium dyes to the *cis*-isomer that is confirmed by several instrumental methods and the regularity of properties with respect to the substituent constants. It was found that the stronger electron-releasing substituent has a more prominent effect on the observed photostability. The changes in the reaction rate of the *trans*-*cis* photoisomerization are successfully correlated with the Hammett constants.

Moreover, the hemicyanine dyes with an electron acceptor and an electron donor group on opposite sides of a  $\pi$  system exhibit an ICT character in solvents of variable polarity. The solvatochromism of dyes under study exhibited regular changes. We observed the blue-shifted absorption and red-shifted emission of the hemicyanine dyes with increasing polarity of solvent. The observed fluorescent behavior was ascribed to ICT upon excitation. An increase in the polarity of solvent decreases the activation barrier and enhances the process.

## Acknowledgements

This work was supported by the Ministry of Science and Higher Education (MNiSW) (grant No 9/2014) and by PL-Grid Infrastructure. Robert Zalesny is grateful to the project Mobilities – enhancing research, science and education at the Matej Bel University (ITMS code: 26110230082, under the Operational Program Education financed by the European Social Fund). The authors express their gratitude to Professor Marek Józefowicz for the assistance in the measurements and to Dr Miroslav Medved for reading the manuscript.

## References

- Q. Zhong, L. Chen, Y. Yang, Y. Cui, G. Qian and M. Wang, Synthesis and Spectroscopic Properties of Conjugated Triphenylaminosubstituted Chromophores, *Dyes Pigm.*, 2008, **76**, 677.
- J. Ostrauskaite, H. R. Karickal, A. Leopold, D. Haarer and M. Thelakkat, Poly[bis(triphenylamine)ether]s with Low Glass Transition Temperatures as Photoconductors in Fact Photorefractive Systems, *J. Mater. Chem.*, 2002, **12**, 58.
- Y. Yasuda, T. Kamiyama and Y. Shiota, Ionic Conductivities of Low Molecular Weight Organic Gels and Their Application as Electrochromic Materials, *Electrochim. Acta*, 2000, **45**, 1537.
- J. P. Chen, H. Tanabe, X.-C. Li, T. Thoms, Y. Okamura and K. Ueno, Novel Organic Hole Transport Material with Very High Tg for Light-Emitting Diodes, *Synth. Met.*, 2003, **132**, 173.
- I. Reva, L. Lapinski, N. Chattopadhyay and R. Fausto, Vibrational Spectrum and Molecular Structure of Triphenylamine Monomer: a Combined Matrix-Isolation FTIR and Theoretical Study, *Phys. Chem. Chem. Phys.*, 2003, **5**, 3844.
- S.-I. Kato, T. Matsumoto, T. Ishi, T. Thiemann, M. Shigeiwa, H. Gorohmaru, S. Maeda, Y. Yamashita and S. Mataka, Strongly Red-Fluorescent Novel Donor- $\pi$ -Bridge-Acceptor- $\pi$ -Bridge-Donor (D- $\pi$ -A- $\pi$ -D) Type 2,1,3-Benzothiadiazoles with Enhanced Two-Photon Absorption Cross-Sections, *Chem. Commun.*, 2004, 2342–2343.
- Y.-T. Chang, S.-L. Hsu, G.-Y. Chen, M.-H. Su, T. A. Singh, E. W.-G. Diao and K.-H. Wei, Intramolecular Donor-Acceptor Regioregular Poly(3-hexylthiophene)s Presenting Octylphenanthrenyl-Imidazole Moieties Exhibit Enhanced Charge Transfer for Heterojunction Solar Cell Applications, *Adv. Funct. Mater.*, 2008, **18**, 2356.
- L. Strekowski, in *Topics in Heterocyclic Chemistry*, ed. R. R. Gupta, Springer, Berlin, Heidelberg, 2008, vol. 14, p. 183.
- R. Walia, M. Hedaitullah, S. F. Naaz, K. Iqbal and H. S. Lamba, Benzimidazole Derivatives – an Overview, *Int. J. Res. Pharm. Chem.*, 2011, **1**, 565.
- M. Boča, R. Boča, G. Kickelbick, W. Linert, I. Svoboda and H. Fuess, Novel Complexes of 2,6-bis(Benzthiazol-2-yl)pyridine, *Inorg. Chim. Acta*, 2002, **338**, 36.
- H. Y. Shrivastava, M. Kanthimathi and B. U. Nair, Copper(II) Complex of a Tridentate Ligand: an Artificial Metalloprotease for Bovine Serum Albumin, *Biochim. Biophys. Acta*, 2002, **1573**, 149.
- V. G. Vaidyanathan and B. U. Nair, Synthesis, Characterization and DNA Binding Studies of a Ruthenium(II) Complex, *J. Inorg. Biochem.*, 2002, **91**, 405.
- R. Vijayalakshmi, M. Kanthimathi, V. Subramanian and B. U. Nair, Interaction of DNA with [Cr(Schiff base)(H<sub>2</sub>O)<sub>2</sub>] ClO<sub>4</sub>, *Biochim. Biophys. Acta*, 2000, **1475**, 157.
- M. N. Hopkinson, C. Richter, M. Schedler and F. Glorius, An Overview of N-Heterocyclic Carbenes, *Nature*, 2014, **510**, 485.
- X. Han, H. Ma and Y. Wang, p-TsOH Catalyzed Synthesis of 2-Arylsubstituted Benzimidazoles, *ARKIVOC*, 2007, **XIII**, 150.
- U. Steiner, M. H. Abdel-Kader, P. Fischer and H. E. A. Kramer, Photochemical *cis/trans* Isomerization of a Stilbazolium Betaine. A Protolytic/Photochemical Reaction Cycle, *J. Am. Chem. Soc.*, 1978, **100**, 3190.
- B. Jędrzejewska, M. Pietrzak and J. Pączkowski, Solvent Effects on the Spectroscopic Properties of Styrylquinolinium Dyes Series, *J. Fluoresc.*, 2010, **20**, 73.
- A. Mishra, G. B. Behera, M. M. G. Krishna and N. Periasamy, Time-Resolved Fluorescence Studies of Aminostyryl Pyridinium Dyes in Organic Solvents and Surfactant solutions, *J. Luminescence*, 2001, **92**, 175.
- H. Jacob, S. Ulrich, U. Jung, S. Lemke, T. Rusch, C. Schutt, F. Petersen, T. Strunskus, O. Magnussen, R. Herges and F. Tuczek, Monitoring the Reversible Photoisomerization of an Azobenzene-functionalized Molecular Triazatriangulene Platform on Au(111) by IRRAS, *Phys. Chem. Chem. Phys.*, 2014, **16**, 22643.
- G. Vantomme and J.-M. Lehn, Reversible Adaptation to Photoinduced Shape Switching by Oligomer-Macrocyclic

- Interconversion with Component Selection in a Three-State Constitutional Dynamic System, *Chem. – Eur. J.*, 2014, **20**, 16188.
- 21 M. Yamamura, K. Yamakawa, Y. Okazaki and T. Nabeshima, Coordination-Driven Macrocyclization for Locking of Photo- and Thermal *cis-trans* Isomerization of Azobenzene, *Chem. – Eur. J.*, 2014, **20**, 16258.
- 22 C. Cernatescu and E. Comanita, Benzazole Derivatives. IV. Reaction of 1,2,3-Trimethylbenzimidazolium Salts with Aromatic Aldehydes, *J. Serb. Chem. Soc.*, 2005, **70**, 1381.
- 23 B. Jędrzejewska, J. Kabatc and J. Pączkowski, 1,3-Bis[4-(*p*-aminostyryl)-pyridinyl]-propane Dibromide Derivatives: Synthesis and Spectroscopic Investigation, *Dyes Pigm.*, 2007, **73**, 361.
- 24 B. Jędrzejewska and A. Rudnicki, The Synthesis and Spectroscopic Investigation of Dichromophoric Hemicyanine Dyes, *Dyes Pigm.*, 2009, **80**, 297.
- 25 J. Olmsted III, Calorimetric Determinations of Absolute Fluorescence Quantum Yields, *J. Phys. Chem.*, 1979, **83**, 2581.
- 26 R. Cammi and B. Mennucci, Linear Response Theory for the Polarizable Continuum Model, *J. Chem. Phys.*, 1999, **110**, 9877.
- 27 S. Chibani, S. Budzak, M. Medved, B. Mennucci and D. Jacquemin, Full cLR-PCM Calculations of the Solvatochromic Effects on Emission Energies, *Phys. Chem. Chem. Phys.*, 2014, **16**, 26024.
- 28 M. J. Frisch, G. W. Trucks, H. B. Schlegel, G. E. Scuseria, M. A. Robb, J. R. Cheeseman, G. Scalmani, V. Barone, B. Mennucci, G. A. Petersson, H. Nakatsuji, M. Caricato, X. Li, H. P. Hratchian, A. F. Izmaylov, J. Bloino, G. Zheng, J. L. Sonnenberg, M. Hada, M. Ehara, K. Toyota, R. Fukuda, J. Hasegawa, M. Ishida, T. Nakajima, Y. Honda, O. Kitao, H. Nakai, T. Vreven, J. A. Montgomery Jr., J. E. Peralta, F. Ogliaro, M. Bearpark, J. J. Heyd, E. Brothers, K. N. Kudin, V. N. Staroverov, R. Kobayashi, J. Normand, K. Raghavachari, A. Rendell, J. C. Burant, S. S. Iyengar, J. Tomasi, M. Cossi, N. Rega, J. M. Millam, M. Klene, J. E. Knox, J. B. Cross, V. Bakken, C. Adamo, J. Jaramillo, R. Gomperts, R. E. Stratmann, O. Yazyev, A. J. Austin, R. Cammi, C. Pomelli, J. W. Ochterski, R. L. Martin, K. Morokuma, V. G. Zakrzewski, G. A. Voth, P. Salvador, J. J. Dannenberg, S. Dapprich, A. D. Daniels, Ö. Farkas, J. B. Foresman, J. V. Ortiz, J. Cioslowski and D. J. Fox, *Gaussian 09, Revision D.01*, Gaussian, Inc., Wallingford CT, 2009.
- 29 L.-Y. Wang, X.-G. Zhang, Y.-P. Shi and Z.-X. Zhang, Microwave-Assisted Solvent-Free Synthesis of Some Hemicyanine Dyes, *Dyes Pigm.*, 2004, **62**, 21.
- 30 L. Wang, X. Zhang, F. Li and Z. Zhang, Microwave-Assisted Solvent-Free Synthesis of Some Styryl Dyes with Benzimidazole Nucleus, *Synth. Commun.*, 2004, **34**, 2245.
- 31 W. A. Schenk, T. Beucke, N. Burzlauff, M. Klüglein and M. Stemmler, The Coordination Chemistry of the C=S Function. XX. Ruthenium Complexes of Thiocinnamaldehydes: Synthesis, Structure and [4 + 2]-Cycloaddition Reactions, *Chem. – Eur. J.*, 2006, **12**, 4821.
- 32 L. Hamdellou, O. Hernandez and J. Meinel, 4-Dimethylamino- $\beta$ -Nitrostyrene and 4-Dimethylamino- $\beta$ -Ethyl- $\beta$ -Nitrostyrene at 100 K, *Acta Crystallogr., Sect. C: Cryst. Struct. Commun.*, 2006, **62**, o557.
- 33 X. H. Zhang, L. Y. Wang, G. H. Zhai, Z. Y. Wen and Z. X. Zhang, X-ray and DFT Studies of the Structure and Spectral Property of 2-[2-(4-Dimethylaminophenyl)ethenyl]-1-methyl-pyridinium Iodide, *J. Mol. Struct.*, 2008, **881**, 117.
- 34 H. Zhou, F. Zhou, P. Wu, Z. Zheng, Z. Yu, Y. Chen, Y. Tu, L. Kong, J. Wu and Y. Tian, Three New Five-Coordinated Mercury (II) Dyes: Structure and Enhanced Two-Photon Absorption, *Dyes Pigm.*, 2011, **91**, 237.
- 35 M. Kong, T. Wang, X. Tian, F. Wang, Y. Liu, Q. Zhang, H. Wang, H. Zhou, J. Wu and Y. Tian, Tunable Two-photon Absorption Near-infrared Materials Containing Different Electron-donors and a  $\pi$ -Bridge Center with Applications in Bioimaging in Live Cells, *J. Mater. Chem. C*, 2015, **3**, 5580.
- 36 J. R. Lakowicz, *Principles of Fluorescence Spectroscopy*, Plenum Press, New York, 2006.
- 37 M. Sauer, J. Hofkens and J. Enderlein, *Handbook of Fluorescence Spectroscopy and Imaging*, WILEY-VCH Verlag GmbH & Co. KGaA, Weinheim, 2011.
- 38 C. Röcker, A. Heilemann and P. Fromherz, Time-Resolved Fluorescence of a Hemicyanine Dye: Dynamics of Rotamerism and Resolution, *J. Phys. Chem.*, 1996, **100**, 12172.
- 39 B. Strehmel, H. Seifert and W. Rettig, Photophysical Properties of Fluorescence Probes. 2. A Model of Multiple Fluorescence for Stilbazolium Dyes Studied by Global Analysis and Quantum Chemical Calculations, *J. Phys. Chem. B*, 1997, **101**, 2232.
- 40 L. L. Zhou, Y. C. Jiang, W. G. Ju, X. H. Zhang and S. K. Wu, Emission Behavior of Non-Planar Intra-Molecular Conjugated Charge Transfer Compounds, *Acta Phys. Chim. Sin.*, 2003, **19**, 670.
- 41 M. Cigán, A. Gáplovský, I. Sigmundová, P. Zahradník, R. Dědic and M. Hromadová, Photostability of D- $\pi$ -A Non-linear Optical Chromophores Containing a Benzothiazolium Acceptor, *J. Phys. Org. Chem.*, 2011, **24**, 450.
- 42 J. Kim and M. Lee, Excited-State Photophysics and Dynamics of a Hemicyanine Dye in AOT Reverse Micelles, *J. Phys. Chem. A*, 1999, **103**, 3378.
- 43 M. Sczepan, W. Rettig, L. Y. Bricks, Y. L. Slominski and A. I. Tolmachev, Unsymmetric Cyanines: Chemical Rigidity and Photophysical Properties, *J. Photochem. Photobiol., A*, 1999, **124**, 75.
- 44 X. Cao, R. W. Tolbert, J. L. McHale and W. D. Edwards, Theoretical Study of Solvent Effects on the Intramolecular Charge Transfer of a Hemicyanine Dye, *J. Phys. Chem. A*, 1998, **102**, 2739.
- 45 R. M. Silverstein, F. X. Webster and D. Kiemle, *Spectrometric Identification of Organic Compounds*, Wiley, 2005.
- 46 A. Mishra, S. Chatterjee and G. Krishnamoorthy, Intramolecular Charge Transfer Emission of trans-2-[4'-(dimethylamino)styryl]benzimidazole: Effect of Solvent and pH, *J. Photochem. Photobiol., A*, 2013, **260**, 50.

- 47 M. Barfield and P. Fagerness, Density Functional Theory/GIAO Studies of the  $^{13}\text{C}$ ,  $^{15}\text{N}$ , and  $^1\text{H}$  NMR Chemical Shifts in Aminopyrimidines and Aminobenzenes: Relationships to Electron Densities and Amine Group Orientations, *J. Am. Chem. Soc.*, 1997, **119**, 8699.
- 48 R. Ditchfield, Self-Consistent Perturbation Theory of Diamagnetism. I. A Gauge-Invariant LCAO Method for N.M.R. Chemical Shifts, *Mol. Phys.*, 1974, **27**, 789.
- 49 K. Woliński, J. F. Hinton and P. Pulay, Efficient Implementation of the Gauge-Independent Atomic Orbital Method for NMR Chemical Shift Calculations, *J. Am. Chem. Soc.*, 1990, **112**, 8251.
- 50 R. Gawinecki, E. Kolehmainen and R. Kauppinen,  $^1\text{H}$  and  $^{13}\text{C}$  NMR Studies of *para*-Substituted Benzaldoximes for Evaluation of the Electron Donor Properties of Substituted Amino Groups, *J. Chem. Soc., Perkin Trans. 2*, 1998, 25.
- 51 T. Cordes, T. Schadendorf, B. Priewisch, K. Rück-Braun and W. Zinth, The Hammett Relationship and Reactions in the Excited Electronic State: Hemithioindigo *Z/E*-Photoisomerization, *J. Phys. Chem. A*, 2008, **112**, 581.
- 52 V. Papper and G. I. Likhtenshtein, Substituted Stilbenes: A New View on Well-Known Systems: New Applications in Chemistry and Biophysics, *J. Photochem. Photobiol., A*, 2001, **140**, 39.
- 53 V. Papper, D. Pines, G. Likhtenshtein and E. Pines, Photophysical Characterization of *trans*-4,4'-Disubstituted Stilbenes, *J. Photochem. Photobiol., A*, 1997, **111**, 87.
- 54 M. B. Smith and J. March, *March's Advanced Organic Chemistry*, Wiley-Interscience, New York, 2001.
- 55 A. Williams, *Free Energy Relationships in Organic and Bio-Organic Chemistry*, The Royal Chemical Society, Cambridge, UK, 2003.
- 56 W. Becker, *Advanced Time Correlated Single Photon Counting Technique*, Springer, New York, 2005.
- 57 R. Lapouyade, K. Czeschka, W. Majenz, W. Rettig, E. Gilibert and C. Rulliere, Photophysics of Donor-Acceptor Substituted Stilbenes. A Time-Resolved Fluorescence Study Using Selectively Bridged Dimethylamino Cyano Model Compounds, *J. Phys. Chem.*, 1992, **96**, 9643.
- 58 E. Abraham, C. Grauby-Heywang, S. Selector and G. Jonusauskas, Characterization of Hemicyanine Langmuir-Blodgett Films by Picosecond Time-Resolved Fluorescence, *J. Photochem. Photobiol., A*, 2008, **93**, 44.